A Merged CYGNSS Soil Moisture Product Using a Minimum Variance Estimator

Erik Hodges, *Member, IEEE*, Clara Chew, *Member, IEEE*, Eric E. Small, *Member, IEEE*, Dinan Bai, *Member, IEEE*, Mohammad Al-Khaldi, *Member, IEEE*, Jeffrey D. Ouellette, *Member, IEEE*, Joel T. Johnson, *Fellow, IEEE*, Fangni Lei, Mehmet Kurum, *Senior Member, IEEE*, Ali Cafer Gurbuz, *Senior Member, IEEE*, Volkan Senyurek, M. M. Nabi, Xiaolan Xu, *Senior Member, IEEE*, Rashmi Shah, *Senior Member, IEEE*, Simon H. Yueh, *Fellow, IEEE*, Akiko Hayashi, Paulo T. Setti Jr., Sajad Tabibi, Emanuele Santi, *Senior Member, IEEE*, Simone Pettinato, *Member, IEEE*, Christopher S. Ruf, *Life Fellow, IEEE*, and Mahta Moghaddam, *Fellow, IEEE*

Received 15 April 2025; revised 1 July 2025; accepted 27 July 2025. Date of publication 11 August 2025; date of current version 26 August 2025. This work was supported in part by the NASA Science Mission Directorate through the University of Southern California under Grant 80LARC21DA003 and the University of Michigan under Contract NNL13AQ00C. An earlier version of this paper was presented in part at IEEE GNSS+R 2023 and in part at the 2024 URSI National Radio Science Meeting [DOI: 10.23919/USNC-URSINRSM60317.2024.10464722]. *(Corresponding author: Erik Hodges.)*

Erik Hodges and Mahta Moghaddam are with the Microwave Systems, Sensors, and Imaging Laboratory (MiXIL), Department of Electrical and Computer Engineering, University of Southern California, Los Angeles, CA 90007 USA (e-mail: ehodges@usc.edu; mahta@usc.edu).

Clara Chew is with Muon Space, Mountain View, CA 94043 USA (e-mail: clara@muonspace.com).

Eric E. Small is with the Department of Geological Sciences, University of Colorado, Boulder, CO 80309 USA (e-mail: eric.small@colorado.edu).

Dinan Bai and Christopher S. Ruf are with the Climate and Space Sciences and Engineering Department and the Remote Sensing Group (RSG), University of Michigan, Ann Arbor, MI 48104 USA (e-mail: dinanbai@umich.edu; cruf@umich.edu).

Mohammad Al-Khaldi and Joel T. Johnson are with the Department of Electrical and Computer Engineering and the ElectroScience Laboratory, The Ohio State University, Columbus, OH 43210 USA (e-mail: al-khaldi.2@osu.edu; johnson.1374@osu.edu).

Jeffrey D. Ouellette is with U.S. Naval Research Laboratory, Washington, DC 20375 USA (e-mail: jeffrey.ouellette@nrl.navy.mil).

Fangni Lei is with the Department of Civil and Environmental Engineering and the Hydrometeorology and Hydrologic Remote Sensing Group, University of Connecticut, Storrs, CT 06269 USA (e-mail: fangni.lei@uconn.edu).

Mehmet Kurum is with the Department of Electrical and Computer Engineering and the Information Processing and Sensing (IMPRESS) Laboratory, University of Georgia, Athens, GA 30602 USA (e-mail: kurum@uga.edu).

Ali Cafer Gurbuz is with the Department of Electrical and Computer Engineering, North Carolina State University, Raleigh, NC 27695 USA (e-mail: aligurbuz@ncsu.edu).

Volkan Senyurek is with the High Performance Computing Collaboratory and the Geosystems Research Institute, Mississippi State University, Starkville, MS 39762 USA (e-mail: volkan@gri.msstate.edu).

M. M. Nabi is with the School of Engineering and Applied Science, Western Kentucky University, Bowling Green, KY 42101 USA (e-mail: mm.nabi@wku.edu).

Xiaolan Xu, Rashmi Shah, Simon H. Yueh, and Akiko Hayashi are with the Jet Propulsion Laboratory, California Institute of Technology, Pasadena, CA 91109 USA (e-mail: Xiaolan.Xu@jpl.nasa.gov; Rashmi.Shah@jpl.nasa.gov; Simon.H.Yueh@jpl.nasa.gov; akiko.k.hayashi@jpl.nasa.gov).

Paulo T. Setti Jr. and Sajad Tabibi are with the Faculty of Science, Technology and Medicine, University of Luxembourg, 4365 Esch-sur-Alzette, Luxembourg (e-mail: paulo.setti@uni.lu; sajad.tabibi@uni.lu).

Emanuele Santi and Simone Pettinato are with the Institute of Applied Physics, National Research Council, 50019 Florence, Italy (e-mail: e.santi@ifac.cnr.it; s.pettinato@ifac.cnr.it).

Digital Object Identifier 10.1109/TGRS.2025.3597532

***Abstract*—Data from the NASA Cyclone Global Navigation Satellite System (CYGNSS) mission have shown promise for the retrieval of soil moisture, and many soil moisture products using CYGNSS data have been developed. In this work, we present a merged product that combines several CYGNSS soil moisture products using a minimum variance estimator (MVE). The MVE identifies an optimal weighted averaging scheme based on the error covariance characteristics of the CYGNSS soil moisture products. The error covariance matrix is computed using two reference datasets: soil moisture data from the Soil Moisture Active Passive (SMAP) radiometer and in situ soil moisture data. The results from each of these provide insights into both the performance of the merged product and the individual input CYGNSS products. Overall, the merged product offers better performance than any individual CYGNSS product while also offering better temporal resolution than SMAP. The results of this work also demonstrate that the use of the MVE is a compelling technique for soil moisture applications.**

***Index Terms*—Geoscience and remote sensing, global navigation satellite system, satellite navigation systems, soil moisture, soil, vehicular and wireless technologies.**

I. Introduction

OBSERVATIONS from spaceborne global navigation satellite system reflectometry (GNSS-R) missions have shown ample sensitivity to soil moisture [1], [2], [3]. Many spaceborne GNSS-R missions have been launched in recent years. These include the TechDemoSat-1 (TDS-1) [4], the U.K. Disaster Monitoring Constellation (U.K.-DMC) [5], the Cyclone Global Navigation Satellite System (CYGNSS) [6], the BuFeng-1 twin satellites [7], and the Spire CubeSats [8]. Of these, CYGNSS has seen the most widespread use in land applications [9].

GNSS-R fills a vital niche in the broader scope of spaceborne soil moisture sensing. Historically, remote sensing of soil moisture has been done by single satellite missions. The current state-of-the-art for L-band microwave remote sensing of soil moisture is the NASA Soil Moisture Active Passive (SMAP) [10] and the European Space Agency (ESA) Soil Moisture and Ocean Salinity (SMOS) [11], which provide high-quality global soil moisture retrievals. However, these missions have a revisit time of up to three days, which may not be sufficient for some applications, such as operational

1558-0644 © 2025 IEEE. All rights reserved, including rights for text and data mining, and training of artificial intelligence and similar technologies. Personal use is permitted, but republication/redistribution requires IEEE permission.
See https://www.ieee.org/publications/rights/index.html for more information.

Authorized licensed use limited to: University of Michigan Library. Downloaded on August 28,2025 at 02:12:38 UTC from IEEE Xplore. Restrictions apply.

weather forecasting. Meanwhile, CYGNSS has an average revisit time of 3–7 h, making daily soil moisture retrievals viable for footprints larger than 20 km. This fast revisit time is the result of CYGNSS employing a constellation of eight small satellites rather than a single large satellite. The launching of eight observatories was made possible by the substantially lower cost GNSS-R platforms, which are much smaller and do not require a heavy or power-hungry onboard transmitter. Soil moisture retrieval quality from GNSS-R is expected to further improve as future missions such as the ESA HydroGNSS [12] and the Muon Space small satellite constellation [13] are launched.

The primary mission of CYGNSS is oceanic wind speed retrieval over tropical cyclones. However, CYGNSS currently has widespread use in soil moisture retrieval as well. Many soil moisture products using data from the NASA CYGNSS mission have been developed [14], [15], [16], [17], [18], [19], [20], [21]. In 2022, the CYGNSS land applications working group launched an effort to assess these products. This assessment analyzed the products with respect to in situ soil moisture data and SMAP soil moisture retrievals. The conclusions drawn from the assessment were that no single product appears to outperform the other products in all cases and that a single combined soil moisture product could take advantage of their best features.

In this work, we present a merged CYGNSS soil moisture product. This product is formed by combining multiple, independently developed, CYGNSS soil moisture products using a minimum variance estimator (MVE). As a result of this technique, the merged product outperforms its constituents and rivals SMAP in key performance metrics while providing daily soil moisture retrievals.

A. Overview of Cygnss Soil Moisture Products

This section provides a brief overview of the CYGNSS soil moisture products that have been developed. Two products use a linear regression model to estimate soil moisture. The first of these is the official soil moisture product of the CYGNSS mission [14], [22], which we will henceforth refer to as the "mission product." The second, which we will call "Lux-Reg," was developed at the University of Luxembourg [23]. In both cases, the regression model is trained for every grid cell using spatiotemporally co-located soil moisture retrievals from SMAP and surface reflectivity observations from CYGNSS. The product of [15] uses a time series retrieval (TSR) approach. We will refer to this product as "TSR." One month of CYGNSS data is fed to a system of equations relating the surface reflectivity (which is assumed to be a known function of soil moisture) and normalized bistatic radar cross section (NBRCS). The model assumes that the effects of vegetation and surface roughness are constant over the duration of the time series such that they cancel out and are removed from the equations. Since the system of equations is not full rank, it is constrained by imposing a monthly maximum and minimum soil moisture derived from historical SMAP soil moisture data. The surface reflectivity is then converted to soil moisture using Peplinski et al.'s soil dielectric model [24]. The product of [19] uses semiempirical modeling (SEM), in which empirical matchups are used to derive inputs to physical models. Unlike some other products, the model is not calibrated by geographic location. Rather, the data are binned according to incidence angle, soil moisture, and vegetation water content (VWC). We will refer to this product as "SEM."

Several products utilizing neural networks have also been developed. Two such products [17], [18] use artificial neural network (ANN)s to convert CYGNSS observed peak reflectivity, trailing edge slope (TES), and incidence angle to soil moisture. These products are trained using soil moisture from the NASA SMAP mission. Both products also utilize an extensive suite of ancillary data, including soil texture, surface water, normalized difference vegetation index (NDVI), and land cover type. The two products differ in the soil moisture training data that are used. Senyurek et al. [18] are trained with in situ data from the International Soil Moisture Network (ISMN), while Lei et al. [17] are trained with remote sensing soil moisture data from SMAP. These two products are not used in the merged product because a successor to them was later developed [16]. The successor product is trained with SMAP and utilizes a convolutional neural network (CNN) that takes the full delay-Doppler map (DDM) of CYGNSS as an input rather than just the peak reflectivity. We will refer to this product as "CNN." Yet, another ANN product [20] uses a broader array of CYGNSS observables, including reflectivity, signal-to-noise ratio (SNR), effective isotropic radiated power (EIRP), normalized radar cross section (NRCS), and more. We will refer to this product as "ANN." Finally, the product of [21] uses a CNN approach similar to that of [16]. This product, CNN, and ANN all use SMAP soil moisture as their training data.

All of these products provide daily soil moisture retrievals. The majority of the products are gridded on the 36-km SMAP equal area scalable Earth (EASE) grid. The exception to this is the CNN product [16], which uses the 9-km SMAP EASE grid. For the merged product, this product is downsampled to 36 km by performing a simple average of the 16 9-km grid cells that make up a single 36-km cell.

B. Merged Cygnss Soil Moisture Product

The CYGNSS merged product is developed using an MVE [25]. This technique is already used in the CYGNSS ocean wind products, but here is applied here to soil moisture products. The MVE performs a weighted averaging of the soil moisture values provided by the input products. The Rao–Blackwell theorem guarantees that the root-mean-square error (RMSE) of the MVE will be lower than that of any of its inputs. The error covariance matrix of the input products is used to find the weights that minimize the variance of the weighted average soil moisture values.

II. Methodology

A. Minimum Variance Estimator

Here, we provide an overview of the mathematical expressions of the MVE. The derivation outline is given in [25]. We have included an expanded derivation in the Appendix with pertinent linear algebra and tensor calculus needed to make it accessible to the readers and useful to a wider audience.

Authorized licensed use limited to: University of Michigan Library. Downloaded on August 28,2025 at 02:12:38 UTC from IEEE Xplore. Restrictions apply.

The MVE is defined by the following weighted average:

$$u_{mv} = \mathbf{m} \cdot \mathbf{u} \tag{1}$$

where u_{mv} is the merged soil moisture value, $\mathbf{m}$ is a vector containing the weights given to the CYGNSS soil moisture products, and $\mathbf{u}$ is the vector of soil moisture values reported by the CYGNSS soil moisture products.

The MVE revolves around finding the optimal weighting vector $\mathbf{m}$, which can be shown to be

$$\mathbf{m} = -\frac{\lambda}{2}\mathbf{1} \cdot \bar{\mathbf{C}}^{-1} \tag{2}$$

where $\bar{\mathbf{C}}$ is the error covariance matrix for the input products and $\mathbf{1}$ is a vector of ones. λ is given by

$$\lambda = \frac{1}{\sum_i \sum_j C_{ij}^{-1}} \tag{3}$$

where C_{ij}^{-1} are the elements of the matrix $\bar{\mathbf{C}}^{-1}$.

B. Merged Product Overview

Six products outlined in I-A are used in the merged product.

1) **Mission** [14], [22].
2) **TSR** [15], [26].
3) **CNN** [16].
4) **SEM** [19].
5) **Lux-Reg** [23].
6) **ANN** [20].

All of the product providers supplied data for the period September 1, 2019 to September 1, 2021. Two years of data provide ample information for the covariance matrix calculations. September 2019 was chosen as the start date because the most recent change in the CYGNSS processing, which was a switch from 1- to 0.5-Hz reporting, occurred in August 2019. The in situ data used originate from the seven SMAP calibration and validation (cal/val) sites [27] that fall within the CYGNSS latitude range of −38° to +38°, and all ISMN [28], [29], [30], [31], [32], [33], [34], [35], [36], [37], [38], [39], [40], [41], [42], [43], [44], [45], [46], [47], [48], [49], [50], [51], sites within this range.

One item of concern is that the input products are each trained using SMAP soil moisture in one way or another and that the training windows of some products overlap with some or all of the merged product time period as shown in Table I. A major concern is that the estimator may bias itself to products with training periods that overlap the observation period. However, this should not be an issue as long as each product is trained with a large enough dataset to be statistically representative. For example, the ANN product is the most favored product by the estimator as shown in Section III. This product has zero overlap with the merged product observation period. Furthermore, this product also only trains using 1% of the available data in its one-year training window and uses the rest for validation [20]. For other products that do overlap, there are factors that reduce these concerns. The TSR algorithm does not undergo 'training' using SMAP's retrievals. Instead, maximum and minimum soil moisture bounds formed using a historical SMAP record extending from 2017 to 2022 are used to constrain the solution of the retrievals' respective systems of equations. The bounds are in the form of maps that undergo day-to-day variations but no year-to-year variability. The CNN product uses a separately trained neural network for each year of retrievals and omits the current year from training. For example, if the algorithm generates soil moisture for the year 2020, it will train using all SMAP soil moisture retrievals from 2018 to 2022, but omit those from 2020.

TABLE I

DATES RANGES OF SMAP TRAINING DATA USED FOR EACH OF THE INPUT CYGNSS SOIL MOISTURE PRODUCTS. SEVERAL PRODUCTS HAVE TRAINING PERIODS THAT OVERLAP SOME OR ALL OF THE MERGED PRODUCT DATE RANGE OF SEPTEMBER 1, 2019–SEPTEMBER 1, 2021

	Product Training Data Time Windows	
Product	Start Date	End Date
Mission	2018 / 08 / 01	2023 / 11 / 15
TSR	2017 / 01 / 01	2022 / 12 / 31
CNN	2018 / 01 / 01	2022 / 12 / 31
SEM	2017 / 03 / 01	2020 / 03 / 01
Lux-Reg	2018 / 08 / 01	2020 / 07 / 31
ANN	2018 / 08 / 01	2019 / 07 / 31

Figs. 1 and 2 show an evaluation of the input CYGNSS soil moisture products. In Fig. 1, maps of the correlation coefficient of the product soil moisture relative to the SMAP radiometer soil moisture are shown. The time period for the correlation calculation was from September 1, 2019 to September 1, 2021, the same time period as the merged product spans. Several trends can be seen across most of the products. The correlation is typically lower in arid regions such as the Sahara and Arabian Peninsula. The correlation is also lower in heavily vegetated regions such as the Amazon and Congo. Five of the six products show similar patterns, but the ANN product has dramatically higher correlation to SMAP than the other five. This suggests that this product follows the tendencies of SMAP much more closely than the other products, and this fact will be corroborated in Section III.

Global maps of coverage likelihood for each product are shown in Fig. 2. To create these maps, for every day during which SMAP reports a soil moisture retrieval, the algorithm checks if there is a CYGNSS retrieval for that day. The map shows the percentage of the SMAP retrievals with a corresponding CYGNSS retrieval. The map for the ANN product shown in Fig. 2(f) shows 100% coverage everywhere. This indicates that this product will always report data under any conditions in which SMAP reports data, suggesting that it has a quality flag scheme that is equally or less lenient than that of SMAP. In the cases of the other products, it is common for there to be low coverage in heavily vegetated regions and/or mountainous regions. These locations typically result in weak scattered signals which have low SNR. Products that set quality flags requiring a minimum SNR will exhibit these types of patterns.

A key component of this work is selecting the reference soil moisture dataset for the error covariance matrix calculation. There are two options that have been evaluated. Each option has distinct advantages and disadvantages.

Authorized licensed use limited to: University of Michigan Library. Downloaded on August 28,2025 at 02:12:38 UTC from IEEE Xplore. Restrictions apply.

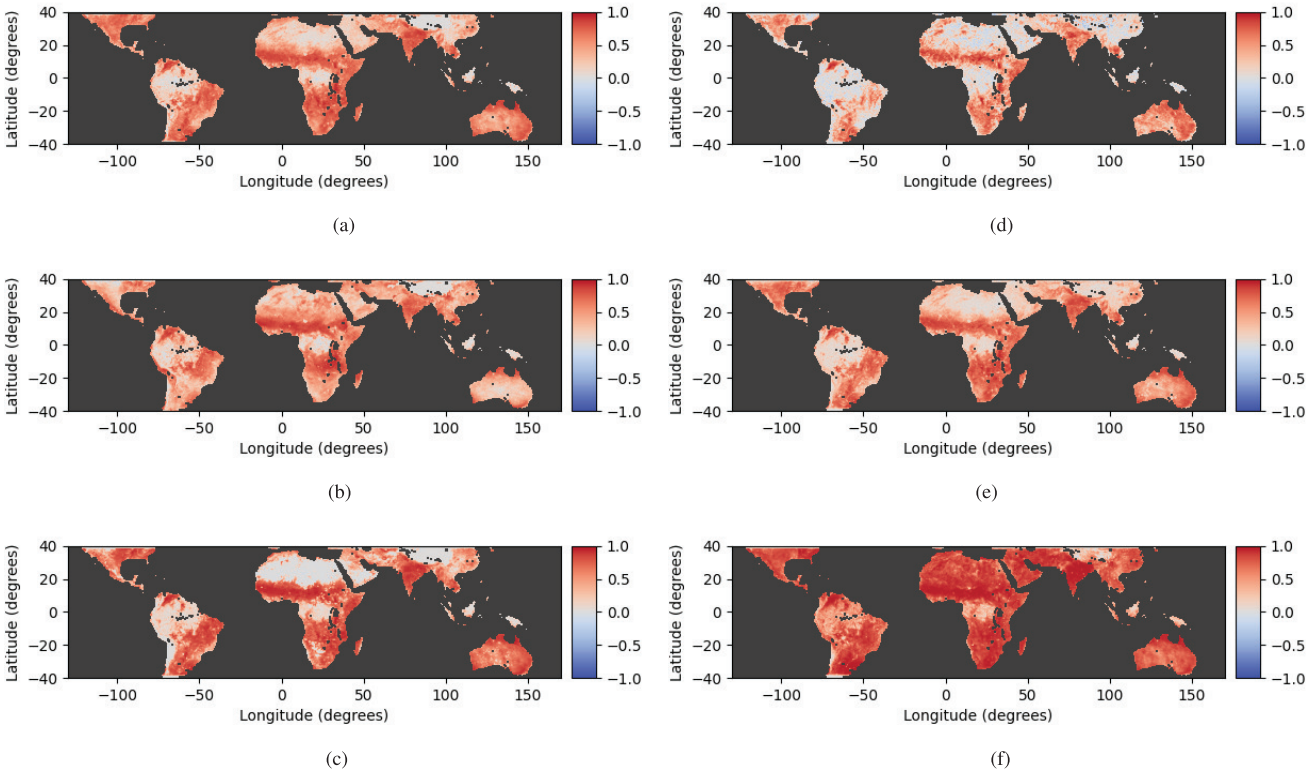


Fig. 1. Maps of the correlation coefficient relative to the SMAP radiometer soil moisture retrievals for each of the CYGNSS products. (a) Mission product. (b) TSR. (c) CNN. (d) SEM. (e) Lux-Reg. (f) ANN.

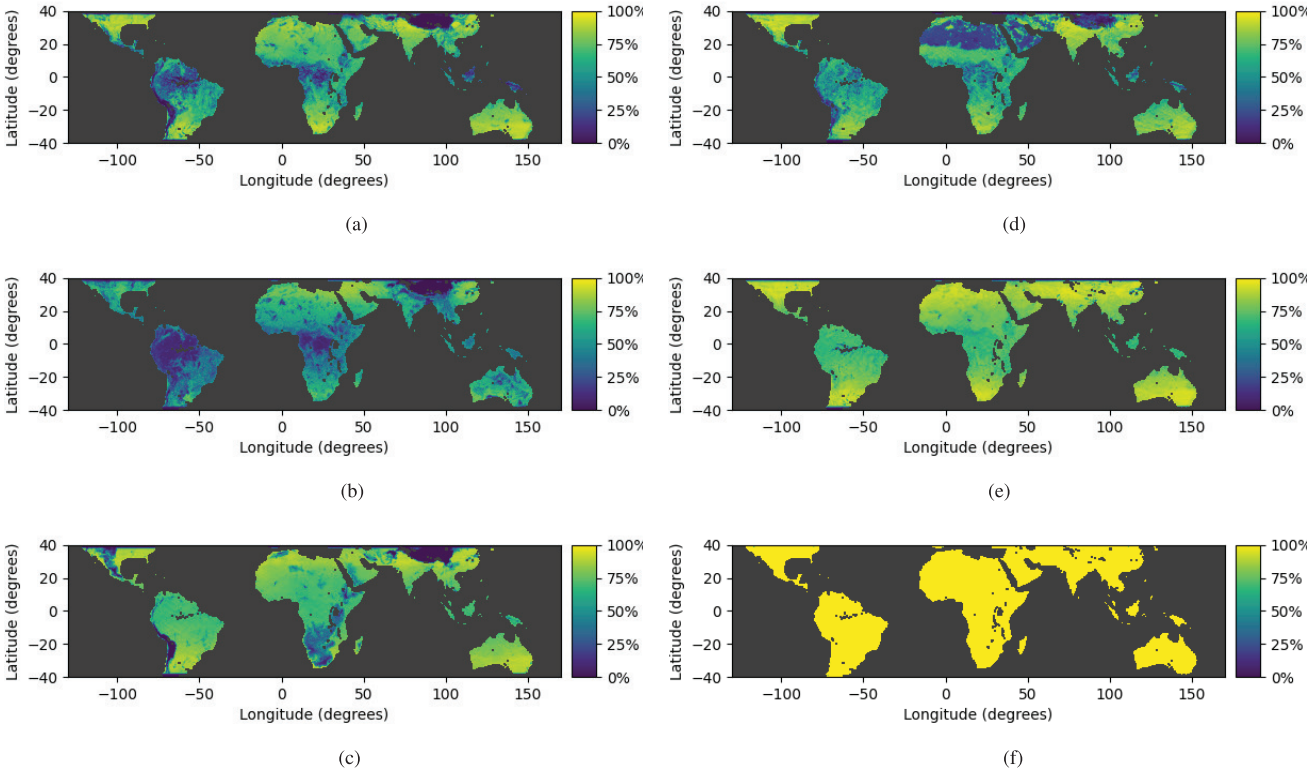


Fig. 2. Maps of the coverage of each product relative to that of SMAP for the period September 1, 2019–September 1, 2021. Each pixel represents the percentage of the total SMAP observations that had an observation from the CYGNSS product for that day. (a) Mission product. (b) TSR. (c) CNN. (d) SEM. (e) Lux-Reg. (f) ANN.

1) In situ soil moisture from the SMAP cal/val sites and ISMN.
2) Soil moisture from the 36-km SMAP L3 Radiometer data (SPL3SMP).

Authorized licensed use limited to: University of Michigan Library. Downloaded on August 28,2025 at 02:12:38 UTC from IEEE Xplore. Restrictions apply.

In situ data have the advantage of unambiguously representing ground conditions at a particular point location. As such, the merged product will be trained to converge to the actual soil moisture. However, there are several issues that must be acknowledged. First, the merged product reports on a 36-km grid, and the in situ data are from point sources. This may introduce a significant error due to sparse sampling of the 36-km grid cells. The amount of in situ data available is also an issue. The soil moisture sensors available only sample a small fraction of the globe. Additionally, there is the issue of representativeness of land cover types. The sites within the CYGNSS latitude zone have a disproportionately large number of cropland and grassland sites compared to all other land cover types. The other issue is that these in situ data must also be used for validating the merged product.

Using the 36-km SMAP Radiometer soil moisture has both advantages and disadvantages compared to using in situ data. First, the grid used by SMAP is the same that is used by the merged product, meaning that there is no error introduced by spatial sampling. Second, SMAP covers the entire globe and provides much more data with which to train the merged product. However, there are some disadvantages of using SMAP. First, SMAP is a soil moisture product retrieved using a model and various assumptions, not a ground truth dataset. Using SMAP as a reference may lead to a merged product that exhibits similar performance shortcomings to SMAP. This issue is compounded by the fact that all of the input CYGNSS soil moisture products use SMAP as training data in one way or another. This could lead to a case where a CYGNSS product that is overfitting to SMAP is given a disproportionately large weighting by the MVE.

The merged product will report "nodata" for a given grid cell unless at least two input products report data. The MVE for the set of all six products is invalid if any of the inputs are missing. Therefore, an MVE is computed for every possible combination of products and the correct averaging scheme is selected on a cell-by-cell basis. This can be done very efficiently using a hash table.

C. Partitioning Using Ancillary Data

An effort was made to improve the results of the merged product by partitioning the data. This took both the reference soil moisture used for covariance calculation and the input soil moisture values from the CYGNSS products and divided them into categories based on ancillary data of either precipitation or vegetation. To form the MVE using the partitioning, both the reference and retrieved soil moisture values were separated into two categories based on the ancillary data. Then, two separate MVEs were generated for each category. The merged product would choose the appropriate MVE on a location-by-location basis by referencing the ancillary data. There were two partitioning approaches used.

The first approach used precipitation data from the global precipitation measurement (GPM) Integrated Multi-satellitE Retrievals for GPM (IMERG) dataset. The goal of this was to divide the data into periods where the soil is expected to be very wet and periods when the soil is expected to be dry. The categories were as follows.

1) *Wet:* Precipitation of at least 1 cm over the prior 48 h.
2) *Dry:* Precipitation of less than 1 cm over the prior 48 h.

The second approach used NDVI data from Moderate Resolution Imaging Spectroradiometer (MODIS) to divide the data into regions of high and low vegetation. The categories were as follows.

1) *Heavy Vegetation:* NDVI of 0.5–1.
2) *Light Vegetation:* NDVI less than 0.5.

Neither partitioning approach resulted in significant changes in the outcomes of the evaluation because the MVE weights were similar for the partitions. The reason for this was that the performance changes for all of the input CYGNSS soil moisture products for various conditions were highly correlated. When the error performance of all of the products is biased similarly, the MVE weights change very little from their previous values, resulting in almost no difference in product performance. For this reason, no further discussion of the partitioned results is provided in what follows.

III. Results

In this section, we present two versions of the merged product. The difference between the two versions is the reference soil moisture dataset used to calculate the error covariance matrix of the MVE. For one version, soil moisture retrievals from SMAP are used. For the other, in situ soil moisture data is used.

A. Covariance Matrices and Product Weighting

Two covariance matrices were generated using the approach detailed in Section II-A. For each, a different reference soil moisture dataset was used. Results using the SMAP 36-km Level 3 Radiometer soil moisture product [52] are presented in Tables II and III. Results using in situ data from the SMAP Core Cal/Val Sites [27] and the ISMN [28], [29], [30], [31], [32], [33], [34], [35], [36], [37], [38], [39], [40], [41], [42], [43], [44], [45], [46], [47], [48], [49], [50], [51] are presented in Tables IV and V.

Each of these reference datasets has limitations that must be acknowledged. The SMAP soil moisture retrievals suffer from a significant amount of error. Validation efforts show an overall unbiased root-mean-square error (ubRMSE) of 0.04 m^3/m^3 [53]. Additionally, the performance of SMAP is dependent on land cover, and the performance is degraded significantly in regions with dense vegetation [53], [54]. The in situ soil moisture data have the advantage of providing high-accuracy soil moisture measurements. However, these data suffer from uncertainty due to spatial sampling. This is not a major concern for the SMAP core cal/val sites, which consist of mutiple sensor nodes distributed to provide a representative sampling of a single 36-km grid cell [27]. However, only seven of these sites exist within the latitude coverage of CYGNSS, so these sites alone do not provide sufficient data to train the estimator. For this reason, data from the ISMN are also used. These data come from independent sensor operators and do not representatively sample the 36-km grid cells since each site consists of either a single sensor or several sensors located within a few kilometers of each other. Since data are collected

Authorized licensed use limited to: University of Michigan Library. Downloaded on August 28,2025 at 02:12:38 UTC from IEEE Xplore. Restrictions apply.

TABLE II

MODIFIED COVARIANCE MATRIX USING SMAP AS THE REFERENCE. THIS IS NOT THE RAW COVARIANCE MATRIX GENERATED BY THE ESTIMATOR. RATHER, IT IS OPERATED ON TO PROVIDE INTUITION. THE DIAGONAL TERMS ARE THE STANDARD DEVIATION OF THE DIFFERENCE OF EACH PRODUCT WITH RESPECT TO SMAP IN UNITS OF m^3/m^3. THIS IS EQUIVALENT TO THE RMSD WITH RESPECT TO SMAP. THE OFF-DIAGONAL TERMS ARE UNITLESS CORRELATION COEFFICIENTS OF THE DIFFERENCES OF EACH PAIR OF PRODUCTS WITH RESPECT TO SMAP

	Mission	TSR	CNN	SEM	Lux-Reg	ANN
Mission	0.075	0.39	0.44	0.31	0.48	0.28
TSR		0.078	0.71	0.55	0.72	0.60
CNN			0.066	0.44	0.81	0.60
SEM				0.129	0.46	0.46
Lux-Reg					0.071	0.58
ANN						0.063

TABLE III

WEIGHTS GIVEN TO EACH PRODUCT WHEN SMAP IS USED AS THE REFERENCE. TEST CASES ARE SHOWN WHERE ONE PRODUCT IS MISSING. NOTE: DUE TO ROUNDING, SOME WEIGHT VECTORS DO NOT SUM EXACTLY TO 1

	Missing Product						
	None	Mission	TSR	CNN	SEM	Lux-Reg	ANN
Mission	0.32		0.32	0.34	0.31	0.31	0.36
TSR	0.01	0.02		0.06	-0.03	0.01	0.13
CNN	0.26	0.37	0.26		0.27	0.25	0.47
SEM	-0.06	-0.04	-0.06	-0.06		-0.06	-0.02
Lux-Reg	-0.02	0.10	-0.01	0.12	0.02		0.05
ANN	0.49	0.54	0.49	0.54	0.47	0.49	

TABLE IV

MODIFIED COVARIANCE MATRIX USING IN SITU SOIL MOISTURE DATA AS THE REFERENCE. THIS IS NOT THE RAW COVARIANCE MATRIX GENERATED BY THE ESTIMATOR. RATHER, IT IS OPERATED ON TO PROVIDE INTUITION. THE DIAGONAL TERMS ARE THE STANDARD DEVIATION OF THE DIFFERENCE OF EACH PRODUCT WITH RESPECT TO THE IN SITU DATA IN UNITS OF m^3/m^3. THIS IS EQUIVALENT TO THE RMSD WITH RESPECT TO THE IN SITU DATA. THE OFF-DIAGONAL TERMS ARE UNITLESS CORRELATION COEFFICIENTS OF THE DIFFERENCES OF EACH PAIR OF PRODUCTS WITH RESPECT TO THE IN SITU DATA

	Mission	TSR	CNN	SEM	Lux-Reg	ANN
Mission	0.109	0.74	0.71	0.69	0.91	0.76
TSR		0.082	0.79	0.88	0.86	0.75
CNN			0.079	0.70	0.87	0.72
SEM				0.078	0.82	0.72
Lux-Reg					0.087	0.75
ANN						0.087

from only a specific location within the 36 km cell, a large uncertainty of the overall soil moisture within the cell exists. Another limitation of using the in situ soil moisture as the reference is that the overwhelming majority of sites are located in low-vegetation regions, which could potentially skew the results.

Both SMAP and the in situ soil moisture have temporal resolutions that are different from the CYGNSS soil moisture products, which report daily soil moisture retrievals. SMAP has a revisit time of 2–3 days but reports soil moisture retrievals at both 6 A.M. and 6 P.M. local solar time (LST). We consider a temporal matchup between SMAP and the CYGNSS products if the SMAP retrieval falls within the time period of 00:00 and 23:59 UTC for the given day. The in situ soil moisture data have a variety of different reporting intervals. For this case, all of the in situ soil moisture measurements within the 24-h period are averaged. Additionally, only sensors with a depth of less than 10 cm were used because L-band signals do not penetrate deeply into soil.

The results shown in Tables II and IV are derived from the error covariance matrices. This format provides much better intuition of the results than the raw covariance matrix. For the diagonal terms, the square root of the error variance was taken. The result of this is that the diagonal terms are the root-mean-square difference (RMSD) of each product. In Table IV, the diagonal terms can be considered as an assessment of each product's performance with respect to the in situ soil moisture data. For the off-diagonal terms, the error correlation

Authorized licensed use limited to: University of Michigan Library. Downloaded on August 28,2025 at 02:12:38 UTC from IEEE Xplore. Restrictions apply.

TABLE V

WEIGHTS GIVEN TO EACH PRODUCT WHEN IN SITU DATA ARE USED AS THE REFERENCE. TEST CASES ARE SHOWN WHERE ONE PRODUCT IS MISSING. NOTE: DUE TO ROUNDING, SOME WEIGHT VECTORS DO NOT SUM EXACTLY TO 1

	Missing Product						
	None	Mission	TSR	CNN	SEM	Lux-Reg	ANN
Mission	-0.06		-0.05	-0.11	-0.19	-0.05	-0.04
TSR	0.03	0.02		0.18	0.12	0.03	0.05
CNN	0.48	0.48	0.48		0.46	0.48	0.49
SEM	0.47	0.48	0.47	0.46		0.47	0.48
Lux-Reg	0.02	-0.04	0.03	0.26	0.47		0.03
ANN	0.07	0.05	0.07	0.20	0.14	0.03	

coefficients are shown. Half of the off-diagonal terms are omitted for clarity since the matrix is symmetric.

Tables III and V show the weighting vectors provided by the MVE. Since it is common for one or more products to be missing for a given acquisition, weighting vectors with one product missing are shown as well.

B. Performance Analysis

The merged product has been analyzed based on the International Geosphere-Biosphere Program (IGBP) land cover type taken from the MODIS 0.5° land cover type dataset [55]. The 17 IGBP land cover classes are separated into seven categories.

1) *Forests (Eight Sites):*
   a) Evergreen needleleaf forest.
   b) Evergreen broadleaf forest.
   c) Deciduous needleleaf forest.
   d) Deciduous broadleaf forest.
   e) Mixed forest.
2) *Shrublands (Six Sites):*
   a) Closed shrublands (>60% coverage).
   b) Open shrublands (10%–60% coverage).
3) *Savannahs (16 Sites):*
   a) Woody savannah (tree cover 30%–60%).
   b) Savannah (tree cover 10%–30%).
4) *Grasslands (84 Sites):*
   a) Grassland.
5) *Croplands (135 Sites):*
   a) Croplands (>60% of area is cultivated).
   b) Cropland and natural mosaic (40%–60% of area is cultivated).
6) *Barren (13 Sites):*
   a) Barren (no vegetation).
7) *Other (Not Used):*
   a) Wetlands.
   b) Urban and built-up lands.
   c) Water bodies.

For each land cover category, the RMSE, ubRMSE, bias, and correlation coefficient were computed. This was done for both the merged product that uses SMAP as its reference and the merged product that uses the average of the CYGNSS products as its reference. The 36-km soil moisture of the SMAP L3 radiometer is also included in these results for comparison purposes. The charts in Tables VI–IX show the

TABLE VI

PRODUCT RMSE BASED ON IGBP LAND COVER CLASS. THE UNITS ARE SOIL MOISTURE VOLUME FRACTION m^3/m^3

Land Cover Class	Merged In Situ Ref	Merged SMAP Ref	SMAP
Forest	0.121	0.132	0.138
Shrubland	0.041	0.044	0.049
Savannah	0.112	0.142	0.143
Grassland	0.063	0.066	0.067
Cropland	0.088	0.094	0.098
Barren	0.067	0.083	0.084

TABLE VII

PRODUCT UBRMSE BASED ON IGBP LAND COVER CLASS. THE UNITS ARE SOIL MOISTURE VOLUME FRACTION m^3/m^3

Land Cover Class	Merged In Situ Ref	Merged SMAP Ref	SMAP
Forest	0.081	0.081	0.071
Shrubland	0.041	0.032	0.037
Savannah	0.053	0.046	0.062
Grassland	0.040	0.038	0.040
Cropland	0.054	0.052	0.057
Barren	0.014	0.019	0.023

TABLE VIII

PRODUCT BIAS BASED ON IGBP LAND COVER CLASS. THE UNITS ARE SOIL MOISTURE VOLUME FRACTION m^3/m^3

Land Cover Class	Merged In Situ Ref	Merged SMAP Ref	SMAP
Forest	-0.002	0.064	0.061
Shrubland	0.015	0.026	0.025
Savannah	0.027	0.083	0.077
Grassland	0.003	0.013	0.010
Cropland	0.009	0.008	0.016
Barren	0.034	0.057	0.055

Authorized licensed use limited to: University of Michigan Library. Downloaded on August 28,2025 at 02:12:38 UTC from IEEE Xplore. Restrictions apply.

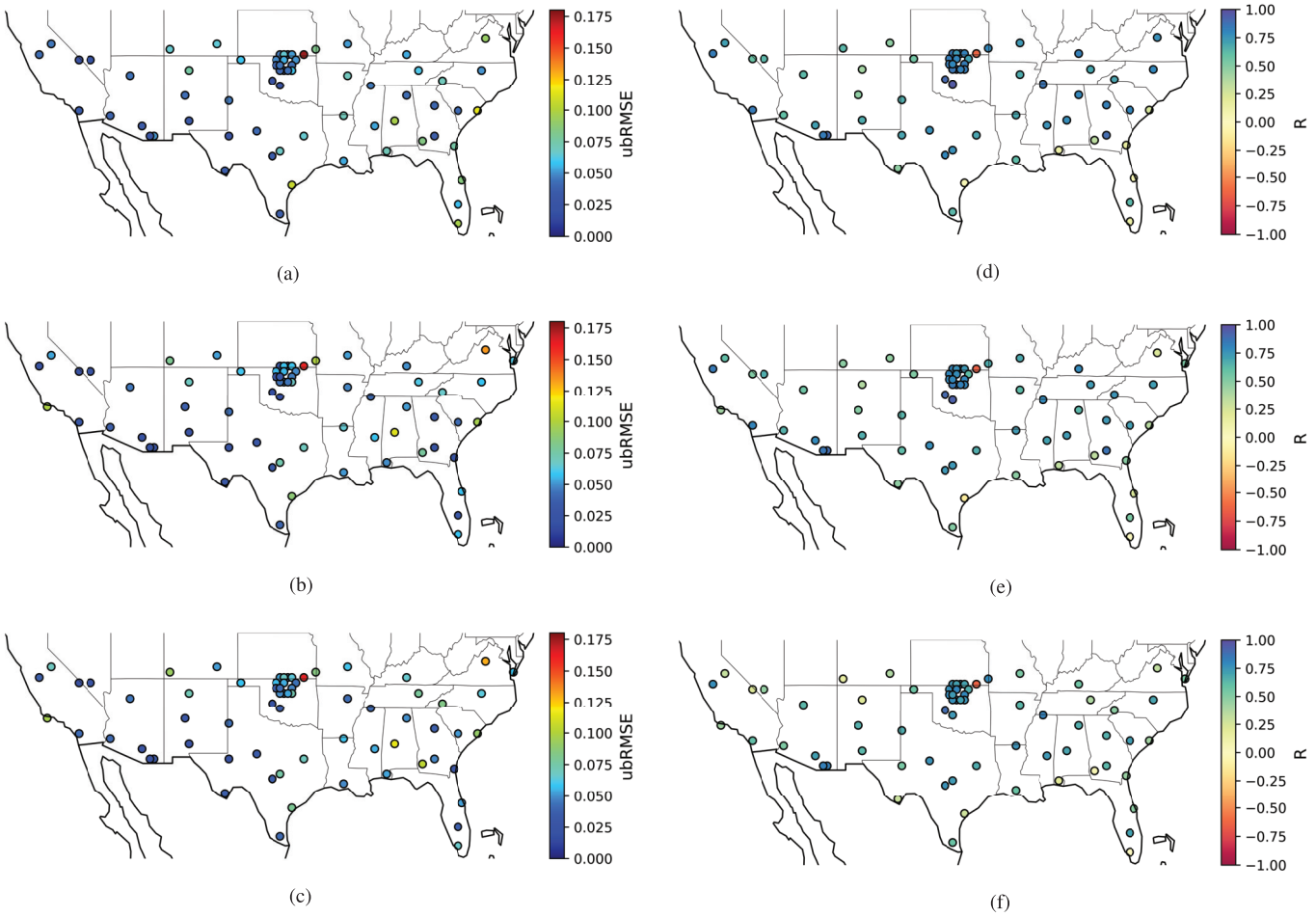


Fig. 3. Maps of ubRMSE (left column) and correlation coefficient (right column) for in situ sites within the contiguous United States. (a) SMAP radiometer. (b) CYGNSS merged product—SMAP reference. (c) CYGNSS merged product—in situ reference. (d) SMAP radiometer. (e) CYGNSS merged product—SMAP reference. (f) CYGNSS merged product—in situ reference.

TABLE IX
PRODUCT CORRELATION COEFFICIENT BASED ON IGBP LAND COVER CLASS

Land Cover Class	Merged In Situ Ref	Merged SMAP Ref	SMAP
Forest	0.434	0.510	0.435
Shrubland	0.659	0.693	0.663
Savannah	0.272	0.258	0.401
Grassland	0.617	0.599	0.610
Cropland	0.620	0.552	0.595
Barren	0.294	0.181	0.054

results of this assessment. The results show that the two merged products have comparable performance to SMAP in most cases. The merged product shows improved RMSE and Bias compared to SMAP for the forest sites.

Maps of ubRMSE and correlation coefficient for both the SMAP L3 radiometer product and the CYGNSS merged products over the in situ sites in the contiguous United States are presented in Fig. 3. The ubRMSE result shows similar performance trends between SMAP and the CYGNSS merged products. Across all three products, ubRMSE values tend to be lower in the drier and more sparsely vegetated western USA than in the more densely vegetated eastern USA. This corroborates the results of the land-cover-based performance analysis. However, there are a small number of sites where the merged products report similar performance, but the performance of SMAP is distinct. The maps of correlation coefficient show that the SMAP radiometer product and the SMAP-referenced merged product exhibit very similar patterns of performance. However, the in situ-referenced merged product differs considerably from the other two at a significant number of sites. From these results, we observe that the spatial variation of ubRMSE is very similar for the two merged products. However, this is not the case for the correlation coefficient, with the SMAP-referenced merged product exhibiting spatial variation similar to that of SMAP, while the in situ-referenced merged product differs from these two.

IV. DISCUSSION

Table III demonstrates that, when SMAP is used as the reference, the ANN product receives the highest weight by far. This can be explained by observing the modified covariance matrix of Table II. The MVE will more heavily weigh products with lower RMSD since this will reduce the error of the merged product. It will also more heavily weigh pairs of

Authorized licensed use limited to: University of Michigan Library. Downloaded on August 28,2025 at 02:12:38 UTC from IEEE Xplore. Restrictions apply.

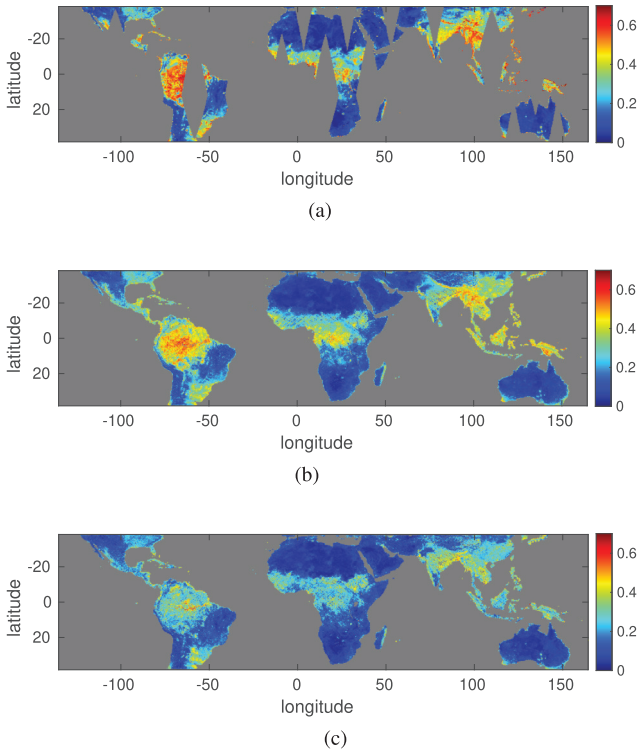


Fig. 4. Global maps of soil moisture (m^3/m^3) from September 1, 2019. Maps of the SMAP radiometer product and both CYGNSS merged products are shown. (a) SMAP radiometer. (b) CYGNSS merged product—SMAP reference. (c) CYGNSS merged product–in situ reference.

products with low correlation to each other, since their errors are more likely to cancel out, thus reducing the error in the merged product. The ANN product has the lowest RMSD in this case, which is why it is given the greatest weight. The Mission product does not have one of the lowest RMSD values, but it has relatively low correlation to the ANN product, which is why it also receives a higher weight than other products with lower RMSD.

Table V demonstrates that, when in situ data are used as the reference, the highest weights are given to CNN and SEM. This is explained in Table IV because these products have the two lowest RMSD values with respect to in situ data and their errors exhibit low correlation relative to other pairs of products. An interesting result in comparing Table IV to Table II is that using in situ data as the reference results in universally higher error correlation. This indicates that some products track SMAP much more closely than others, whereas all six products seem to track the in situ data similarly. It is notable that the ANN product has very low weight when in situ data are used as reference. As this product tracks SMAP closely, it also manifests some of the performance shortcomings of SMAP. This is corroborated in Fig. 4, which shows an example of the merged product for a specific day (September 1, 2019) for both reference datasets, as well as the SMAP L3 radiometer soil moisture product for that day. In the SMAP reference case, where ANN has a large weight, the soil moisture values in forested regions such as the Amazon, the Congo, and Southeast Asia are much higher than those in the in situ reference case, where ANN has a lower weight. This is notable because SMAP often overestimates soil moisture in forested areas [54] and the SMAP-referenced merged product shows soil moisture much closer to SMAP in these regions. The in situ reference merged product is closer to the true soil moisture value in these forested regions.

It is helpful to reiterate that a disadvantage of using in situ soil moisture data as the reference is that the merged product is reported on a 36 km grid, while the sensors of ISMN [28], [29], [30], [31], [32], [33], [34], [35], [36], [37], [38], [39], [40], [41], [42], [43], [44], [45], [46], [47], [48], [49], [50], [51] are point measurements. This creates an error source since a point measurement is assumed to represent the soil moisture of the entire 36-km grid cell. The perceived limitations associated with in situ gauge networks are less severe in the case of SMAP's cal/val sites given their more dense spatial sampling [27]. However, the available ISMN sites vastly outnumber the SMAP cal/val sites. It should also be noted that Fig. 3 shows the in situ reference product having better overall performance than the SMAP reference product. This comparative result is expected since the in situ reference product is optimized to minimize error with respect to these sites. However, this should not be taken as a condemnation of the validity of this version of the product. After all, the estimator simply performs a weighted average of CYGNSS-derived products that do not use the in situ data for training whatsoever.

Overall, the merged product provides a soil moisture dataset with better performance than any CYGNSS product, and improved temporal resolution compared to SMAP, providing daily soil moisture retrievals. One key feature of using the MVE for soil moisture is that the estimator becomes more effective as the diversity of the input products increases. This will be particularly important because many future GNSS-R missions are planned or are in progress, including the SPIRE Cubesats [8], smallsats from MuonSpace [13], and the ESA HydroGNSS mission [12]. The MVE can be used to combine products from one or more of these missions and CYGNSS to produce a soil moisture product with even better performance.

V. Conclusion

Overall, the CYGNSS merged product is a promising development in GNSS-R soil moisture retrieval. It demonstrates that performance similar to flagship microwave soil moisture sensing missions is possible while leveraging the improved temporal resolution enabled by constellations of GNSS-R receivers. The results of this work demonstrate that using an MVE for combining multiple soil moisture products shows great promise for future applications. The two reference datasets tested, SMAP and in situ soil moisture data, both have advantages and disadvantages. Using SMAP provides a greater volume of data and avoids error due to the resolution mismatch between the remote sensing and in situ data. Using in situ soil moisture as the reference results in more realistic soil moisture retrievals over forested regions.

Future merged products can improve on these results by leveraging additional data from future GNSS-R missions. Additionally, several CYGNSS soil moisture products have a 9-km spatial resolution, meaning that it is possible to develop

Authorized licensed use limited to: University of Michigan Library. Downloaded on August 28,2025 at 02:12:38 UTC from IEEE Xplore. Restrictions apply.

a second merged product with this improved resolution. Doing so would also have the benefit of reducing the resolution mismatch between the product and in situ data.

APPENDIX
MVE DERIVATION

The following derivation follows the procedure found in the appendix of [25]. However, the derivation of [25] is abbreviated and assumes that the reader has knowledge of several advanced mathematical processes. Here, we present an in depth mathematical derivation with explanations of all steps. In the following derivation, scalar quantities are represented in regular font, vector quantities are represented in bold font, and 2-D tensor quantities are represented in uppercase bold font with a bar.

To begin, we represent the weighted averaging as

$$u_{mv} = \mathbf{m} \cdot \mathbf{u} \tag{4}$$

where u_{mv} is the merged soil moisture value, $\mathbf{m}$ is the vector of weights, and $\mathbf{u}$ is the vector of input soil moisture values. To find the optimal weights, we require the error covariance matrix of the input products $\bar{\mathbf{C}}$, whose elements are given as

$$C_{ij} = \left\langle (u_i - u_{\text{true}}) \left(u_j - u_{\text{true}}\right) \right\rangle \tag{5}$$

where u_i and u_j are the soil moisture values reported by the ith and jth products, respectively, u_{true} is some reference soil moisture value which we assume to be the true soil moisture, and the angle brackets denote the expected value of a random variable. As this is a *minimum variance* estimator, we must have an expression for the variance of the output soil moisture error that we can minimize. This is given by

$$\sigma_{mv}^2 = \left\langle (u_{mv} - u_{\text{true}})^2 \right\rangle. \tag{6}$$

This problem is solvable via the method of Lagrange multipliers if the following equality holds:

$$\sigma_{mv}^2 = \mathbf{m} \cdot \bar{\mathbf{C}} \cdot \mathbf{m}' \tag{7}$$

where the "prime" operator denotes the transpose of a vector or matrix. We will now prove this equality. We can expand the right-hand side of (7) as follows:

$$\mathbf{m} \cdot \bar{\mathbf{C}} \cdot \mathbf{m}' = \sum_j \left(\sum_i m_i C_{ij} \right) m_j. \tag{8}$$

Next, we substitute the expression for C_{ij} found in (5) to obtain

$$\mathbf{m} \cdot \bar{\mathbf{C}} \cdot \mathbf{m}' = \sum_j \sum_i m_i m_j \langle (u_i - u_{\text{true}}) \left(u_j - u_{\text{true}}\right) \rangle. \tag{9}$$

Distributing the multiplication, we get

$$\mathbf{m} \cdot \bar{\mathbf{C}} \cdot \mathbf{m}' = \sum_j \sum_i \left\langle (m_i u_i - m_i u_{\text{true}}) \left(m_j u_j - m_j u_{\text{true}}\right) \right\rangle. \tag{10}$$

Revisiting (4), we see that $m_i u_i$ and $m_j u_j$ are, respectively, the ith and jth elements of the dot product that is evaluated to obtain u_{mv} in (4). Additionally, since $\mathbf{m}$ is a vector of weights for a weighted average, the sum of its elements must be one. Therefore, we have the following two expressions:

$$u_{mv} = \mathbf{m} \cdot \mathbf{u} = \sum_i m_i u_i \tag{11}$$

$$\sum_i m_i = 1. \tag{12}$$

Now, we consider the sum over i for (10), which allows us to insert the expressions of (11) and (12) to obtain

$$\mathbf{m} \cdot \bar{\mathbf{C}} \cdot \mathbf{m}' = \sum_j \left\langle (u_{mv} - u_{\text{true}}) \left(m_j u_j - m_j u_{\text{true}}\right) \right\rangle. \tag{13}$$

Performing the same steps with the sum over j, we arrive at

$$\mathbf{m} \cdot \bar{\mathbf{C}} \cdot \mathbf{m}' = \left\langle (u_{mv} - u_{\text{true}})^2 \right\rangle = \sigma_{mv}^2 \tag{14}$$

thus proving the equality in (7).

Now that we have a useful expression for σ_{mv}^2, we will use the method of Lagrange multipliers to find the vector of weights $\mathbf{m}$ that minimizes the variance. We cannot solve this by simply setting the gradient of σ_{mv} equal to zero because this yields the trivial solution $\mathbf{m} = \mathbf{0}$. The method of Lagrange multipliers allows us to impose the condition of (12) onto the solution space. We have the following:

$$\nabla_m \left(\mathbf{m} \cdot \bar{\mathbf{C}} \cdot \mathbf{m}' + \lambda \mathbf{m} \cdot \mathbf{1} \right) = 0 \tag{15}$$

where λ is the Lagrange multiplier and $\mathbf{1}$ is a vector of ones. The operator ∇_m indicates the gradient taken with respect to the elements of $\mathbf{m}$. Applying this operator to a vector gives us a 2-D tensor of the following form:

$$[\nabla_m \mathbf{a}]_{ij} = \frac{\partial a_i}{\partial m_j}. \tag{16}$$

We can simplify (15) by observing that

$$\nabla_m \mathbf{m} = \nabla_m \mathbf{m}' = \bar{\mathbf{I}} \tag{17}$$

where $\bar{\mathbf{I}}$ is the identity matrix. This yields

$$\nabla_m \left(\mathbf{m} \cdot C \cdot \mathbf{m}' \right) + \lambda \mathbf{1} = 0. \tag{18}$$

We must now evaluate $\nabla_m(\mathbf{m} \cdot \bar{\mathbf{C}} \cdot \mathbf{m}')$. We will do this by applying the product rule for the gradient of a tensor. First, we will find the gradient of a subsection of this expression, then later substitute it to obtain the full expression. We have the following:

$$\nabla_m \left(\bar{\mathbf{C}} \cdot \mathbf{m}' \right) = \mathbf{m}' \cdot \nabla_m \bar{\mathbf{C}}' + \bar{\mathbf{C}} \cdot \nabla_m m'. \tag{19}$$

It is important to realize that the matrix $\bar{\mathbf{C}}$ is constant, so

$$\nabla_m \bar{\mathbf{C}} = \nabla_m \bar{\mathbf{C}}' = 0. \tag{20}$$

Applying (17) and (20), it is shown that

$$\nabla_m \left(\bar{\mathbf{C}} \cdot \mathbf{m}' \right) = \bar{\mathbf{C}}. \tag{21}$$

We will now use substitution to evaluate $\nabla_m(\mathbf{m} \cdot \bar{\mathbf{C}} \cdot \mathbf{m}')$. We will define

$$\mathbf{z} = \nabla_m \left(\bar{\mathbf{C}} \cdot \mathbf{m}' \right) \tag{22}$$

which gives us

$$\nabla_m \left(\mathbf{m} \cdot \bar{\mathbf{C}} \cdot \mathbf{m}' \right) = \nabla_m \left(\mathbf{m} \cdot \mathbf{z} \right). \tag{23}$$

We can now easily apply the product rule for the gradient of a tensor a second time to evaluate this expression

$$\nabla_m \left(\mathbf{m} \cdot \mathbf{z} \right) = \mathbf{m}' \cdot \nabla_m \mathbf{z}' + \mathbf{z} \cdot \nabla_m m'. \tag{24}$$

Authorized licensed use limited to: University of Michigan Library. Downloaded on August 28,2025 at 02:12:38 UTC from IEEE Xplore. Restrictions apply.

Now, inserting (21) and (22), we obtain

$$\nabla_m \left(\mathbf{m} \cdot \bar{\mathbf{C}} \cdot \mathbf{m}'\right) = \bar{\mathbf{C}} \cdot \mathbf{m}' + \mathbf{m} \cdot \bar{\mathbf{C}}. \tag{25}$$

We also observe that since the error covariance matrix $\bar{\mathbf{C}}$ is symmetric

$$\bar{\mathbf{C}} \cdot \mathbf{m}' = \mathbf{m} \cdot \bar{\mathbf{C}}. \tag{26}$$

Therefore, we can reduce (25) to

$$\nabla_m \left(\mathbf{m} \cdot \bar{\mathbf{C}} \cdot \mathbf{m}'\right) = 2\mathbf{m} \cdot \bar{\mathbf{C}}. \tag{27}$$

Now, we return to the minimization problem. Substituting (27) into (18) gives us the following easily solvable equation

$$2\mathbf{m} \cdot \bar{\mathbf{C}} + \lambda \mathbf{1} = 0. \tag{28}$$

Solving, we obtain the vector of weights $\mathbf{m}$ that minimizes σ_{mv}

$$\mathbf{m} = -\frac{\lambda}{2}\mathbf{1} \cdot \bar{\mathbf{C}}^{-1}. \tag{29}$$

The Lagrange multiplier λ is obtained by applying (12), which forces the sum of the weights to equal one

$$\lambda = \frac{1}{\sum_i \sum_j C_{ij}^{-1}}. \tag{30}$$

ACKNOWLEDGMENT

The authors acknowledge the work of Yeongil Lee and the KIHS_CMC and KIHS_SMC teams in support of the ISMN. They acknowledge the work of Frank Annor and Nicolaas Cornelis van de Giesen and the Trans-African Hydro-Meterological Observatory (TAHMO) Network Community in support of the ISMN. They also acknowledge the work of Ileen de Kat and Richard de Jeu as well as the VDS network team in support of the ISMN. Part of this research was carried out at the Jet Propulsion Laboratory, California Institute of Technology, under a contract with the National Aeronautics and Space Administration (80NM0018D0004).

REFERENCES

[1] H. Carreno-Luengo et al., "The CYGNSS mission: On-going science team investigations," *Remote Sens.*, vol. 13, no. 9, p. 1814, May 2021. [Online]. Available: https://www.mdpi.com/2072-4292/13/9/1814

[2] X. Wu, W. Ma, J. Xia, W. Bai, S. Jin, and A. Calabia, "Spaceborne GNSS-R soil moisture retrieval: Status, development opportunities, and challenges," *Remote Sens.*, vol. 13, no. 1, p. 45, Dec. 2020. [Online]. Available: https://www.mdpi.com/2072-4292/13/1/45

[3] A. Melebari, J. D. Campbell, E. Hodges, and M. Moghaddam, "Analytical assessment of GNSS-R delay Doppler map sensitivity to land surface variables using a physics-based model," *IEEE Trans. Geosci. Remote Sens.*, vol. 63, 2025, Art. no. 2000915.

[4] M. Unwin, S. Duncan, P. Jales, P. Blunt, and J. Tye, "Implementing GNSS-reflectometry in space on the TechDemoSat-1 mission," in *Proc. 27th Int. Tech. Meeting Satell. Division Inst. Navigat. (ION GNSS)*, 2014, pp. 1222–1235.

[5] S. Gleason et al., "Detection and processing of bistatically reflected GPS signals from low Earth orbit for the purpose of ocean remote sensing," *IEEE Trans. Geosci. Remote Sens.*, vol. 43, no. 6, Jun. 2005. [Online]. Available: http://ieeexplore.ieee.org/document/1433022

[6] C. S. Ruf et al., "The CYGNSS nanosatellite constellation hurricane mission," in *Proc. Int. Geosci. Remote Sens. Symp. (IGARSS)*, Aug. 2012, pp. 214–216.

[7] C. Jing, X. Niu, C. Duan, F. Lu, G. Di, and X. Yang, "Sea surface wind speed retrieval from the first Chinese GNSS-R mission: Technique and preliminary results," *Remote Sens.*, vol. 11, no. 24, p. 3013, Dec. 2019. [Online]. Available: https://www.mdpi.com/2072-4292/11/24/3013/htm

[8] V. Freeman et al., "Earth surface monitoring with Spire's new GNSS reflectometry (GNSS-R) CubeSats," in *Proc. EGU Gen. Assem.*, 2020.

[9] C. Ruf et al., "The nasa cyclone global navigation satellite system smallsat constellation," Aug. 2022.

[10] P. O'Neill, D. Entekhabi, E. Njoku, and K. Kellogg, "The NASA soil moisture active passive (SMAP) mission: Overview," in *Proc. IEEE Int. Geosci. Remote Sens. Symp.*, Jul. 2010, pp. 3236–3239.

[11] Y. H. Kerr et al., "The SMOS mission: New tool for monitoring key elements ofthe global water cycle," *Proc. IEEE*, vol. 98, no. 5, pp. 666–687, May 2010.

[12] M. J. Unwin et al., "An introduction to the HydroGNSS GNSS reflectometry remote sensing mission," *IEEE J. Sel. Topics Appl. Earth Observ. Remote Sens.*, vol. 14, pp. 6987–6999, 2021.

[13] D. Masters et al. (2023). *Introduction To the Muon Space Small Satellite Constellation*. [Online]. Available: https://paz.ice.csic.es/documents/2ndWorkshop/DAY2_SESSION1_3_DMasters_MuonSpace.pdf

[14] C. Chew and E. Small, "Description of the UCAR/CU soil moisture product," *Remote Sens.*, vol. 12, no. 10, p. 1558, May 2020.

[15] M. M. Al-Khaldi and J. T. Johnson, "Soil moisture retrievals using CYGNSS data in a time-series ratio method: Progress update and error analysis," *IEEE Geosci. Remote Sens. Lett.*, vol. 19, pp. 1–5, 2022.

[16] M. M. Nabi, V. Senyurek, A. C. Gurbuz, and M. Kurum, "Deep learning-based soil moisture retrieval in CONUS using CYGNSS Delay-Doppler maps," *IEEE J. Sel. Topics Appl. Earth Observ. Remote Sens.*, vol. 15, pp. 6867–6881, 2022.

[17] F. Lei et al., "Quasi-global machine learning-based soil moisture estimates at high spatio-temporal scales using CYGNSS and SMAP observations," *Remote Sens. Environ.*, vol. 276, Jul. 2022, Art. no. 113041. [Online]. Available: https://www.sciencedirect.com/science/article/pii/S0034425722001559

[18] V. Senyurek, F. Lei, D. Boyd, A. C. Gurbuz, M. Kurum, and R. Moorhead, "Evaluations of machine learning-based CYGNSS soil moisture estimates against SMAP observations," *Remote Sens.*, vol. 12, no. 21, p. 3503, Oct. 2020. [Online]. Available: https://www.mdpi.com/2072-4292/12/21/3503

[19] S. H. Yueh, R. Shah, M. J. Chaubell, A. Hayashi, X. Xu, and A. Colliander, "A semiempirical modeling of soil moisture, vegetation, and surface roughness impact on CYGNSS reflectometry data," *IEEE Trans. Geosci. Remote Sens.*, vol. 60, 2022, Art. no. 5800117.

[20] E. Santi et al., "Global soil moisture mapping at 5 km by combining GNSS reflectometry and machine learning in view of HydroGNSS," *Sci. Remote Sens.*, vol. 10, Dec. 2024, Art. no. 100177. [Online]. Available: https://www.sciencedirect.com/science/article/pii/S2666017224000610

[21] T. M. Roberts, I. Colwell, C. Chew, S. Lowe, and R. Shah, "A deep-learning approach to soil moisture estimation with GNSS-R," *Remote Sens.*, vol. 14, no. 14, p. 3299, Jul. 2022. [Online]. Available: https://www.mdpi.com/2072-4292/14/14/3299

[22] D. Bai and C. S. Ruf, "Performance assessment of cygnss v3.2 soil moisture," Tech. Rep.

[23] P. Setti and S. Tabibi, "Comprehensive analysis of CYGNSS GNSS-R data for enhanced soil moisture retrieval," *IEEE J. Sel. Topics Appl. Earth Observ. Remote Sens.*, vol. 18, pp. 663–679, 2025.

[24] N. R. Peplinski, F. T. Ulaby, and M. C. Dobson, "Dielectric properties of soils in the 0.3–1.3-GHz range," *IEEE Trans. Geosci. Remote Sens.*, vol. 33, no. 3, pp. 803–807, May 1995.

[25] M. P. Clarizia, C. S. Ruf, P. Jales, and C. Gommenginger, "Spaceborne GNSS-R minimum variance wind speed estimator," *IEEE Trans. Geosci. Remote Sens.*, vol. 52, no. 11, pp. 6829–6843, Nov. 2014.

[26] J. D. Ouellette, M. M. Al-Khaldi, and J. T. Johnson, "Soil moisture retrieval using CYGNSS data in a time-series ratio method: Progress update and error analysis, part II," *IEEE J. Sel. Topics Appl. Earth Observ. Remote Sens.*, vol. 17, pp. 16426–16432, 2024.

[27] A. Colliander et al. (2017). *SMAP/in Situ Core Validation Site Land Surface Parameters Match-up Data, Version 1*. [Online]. Available: https://nsidc.org/data/NSIDC-0712/versions/1

[28] W. Dorigo et al., "The international soil moisture network: Serving Earth system science for over a decade," *Hydrol. Earth Syst. Sci.*, vol. 25, no. 11, pp. 5749–5804, 2021.

[29] W. A. Dorigo et al., "Global automated quality control of in situ soil moisture data from the international soil moisture network," *Vadose Zone J.*, vol. 12, no. 3, pp. 1–21, Aug. 2013.

[30] T. Pellarin, J. P. Laurent, B. Cappelaere, B. Decharme, L. Descroix, and D. Ramier, "Hydrological modelling and associated microwave emission of a semi-arid region in south-western Niger," *J. Hydrol.*, vol. 375, nos. 1–2, pp. 262–272, Aug. 2009.

Authorized licensed use limited to: University of Michigan Library. Downloaded on August 28,2025 at 02:12:38 UTC from IEEE Xplore. Restrictions apply.

[31] E. Mougin et al., "The AMMA-CATCH gourma observatory site in Mali: Relating climatic variations to changes in vegetation, surface hydrology, fluxes and natural resources," *J. Hydrol.*, vol. 375, nos. 1–2, pp. 14–33, Aug. 2009.
[32] B. Cappelaere et al., "The AMMA-CATCH experiment in the cultivated sahelian area of south-west Niger–investigating water cycle response to a fluctuating climate and changing environment," *J. Hydrol.*, vol. 375, nos. 1–2, pp. 34–51, Aug. 2009.
[33] P. de Rosnay et al., "Multi-scale soil moisture measurements at the gourma meso-scale site in Mali," *J. Hydrol.*, vol. 375, nos. 1–2, pp. 241–252, Aug. 2009.
[34] T. Lebel et al., "AMMA-CATCH studies in the sahelian region of West-Africa: An overview," *J. Hydrol.*, vol. 375, nos. 1–2, pp. 3–13, Aug. 2009.
[35] S. Galle et al., "AMMA-CATCH a hydrological, meteorological and ecological long term observatory on West Africa: Some recent results," in *Proc. AGU Fall Meeting Abstr.*, Dec. 2015.
[36] D. R. Cook. (2016). *Soil Temperature and Moisture Profile (stamp) System Handbook*. [Online]. Available: https://www.osti.gov/biblio/1332724
[37] D. Cook. (2018). *Surface Energy Balance System (SEBS) Instrument Handbook*. [Online]. Available: https://www.osti.gov/biblio/1004944
[38] M. Zreda, D. Desilets, T. P. A. Ferré, and R. L. Scott, "Measuring soil moisture content non-invasively at intermediate spatial scale using cosmic-ray neutrons," *Geophys. Res. Lett.*, vol. 35, no. 21, Nov. 2008.
[39] M. Zreda et al., "COSMOS: The cosmic-ray soil moisture observing system," *Hydrol. Earth Syst. Sci.*, vol. 16, no. 11, pp. 4079–4099, Nov. 2012.
[40] C. Mattar, A. Santamar'ıa-Artigas, C. Durán-Alarcón, L. Olivera-Guerra, R. Fuster, and D. Borvarán, "The LAB-net soil moisture network: Application to thermal remote sensing and surface energy balance," *Data*, vol. 1, no. 1, p. 6, Jun. 2016.
[41] C. Mattar, A. Santamaría-Artigas, C. Durán-Alarcón, L. Olivera-Guerra, and R. Fuster, "Lab-net the first Chilean soil moisture network for remote sensing applications," in *Proc. Quant. Remote Sens. Symp. (RAQRS)*, 2014, pp. 22–26.
[42] Z. Su et al., "The Tibetan Plateau observatory of Plateau scale soil moisture and soil temperature (Tibet-Obs) for quantifying uncertainties in coarse resolution satellite and model products," *Hydrol. Earth Syst. Sci.*, vol. 15, no. 7, pp. 2303–2316, Jul. 2011.
[43] L. Dente, Z. Su, and J. Wen, "Validation of SMOS soil moisture products over the maqu and Twente regions," *Sensors*, vol. 12, no. 8, pp. 9965–9986, Jul. 2012.
[44] A. B. Smith et al., "The Murrumbidgee soil moisture monitoring network data set," *Water Resour. Res.*, vol. 48, no. 7, Jul. 2012.
[45] R. Young et al., "Soil moisture and meteorological observations from the Murrumbidgee catchment," Dept. Civil Environ. Eng., The Univ. Melbourne, Melbourne, VIC, Australia, Tech. Rep., 2008.
[46] G. L. Schaefer, M. H. Cosh, and T. J. Jackson, "The USDA natural resources conservation service soil climate analysis network (SCAN)," *J. Atmos. Ocean. Technol.*, vol. 24, no. 12, pp. 2073–2077, Dec. 2007.
[47] J. Ardö, "A 10-year dataset of basic meteorology and soil properties in central Sudan," *Dataset Papers Geosci.*, vol. 2013, pp. 1–6, Nov. 2013.
[48] G. H. Leavesley et al., "A modeling framework for improved agricultural water supply forecasting," in *Proc. AGU Fall Meeting Abstr.*, vol. 2008, Dec. 2008, pp. 1–14.
[49] G. H. Leavesley et al. (2010). *A Modeling Framework for Improved Agricultural Water-supply Forecasting*. [Online]. Available: https://api.semanticscholar.org/CorpusID:129416417
[50] T. Bongiovanni and T. G. Caldwell, "Texas soil observation network (TxSON)," Univ. Texas at Austin, Austin, TX, USA, Tech. Rep., 2019, doi: 10.18738/T8/JJ16CF.
[51] J. E. Bell et al., "U.S. climate reference network soil moisture and temperature observations," *J. Hydrometeorology*, vol. 14, no. 3, pp. 977–988, Jun. 2013.
[52] P. E. O'Neill, S. Chan, E. G. Njoku, T. Jackson, and R. Bindlish. (2016). *SMAP L3 Radiometer Global Daily 36 Km EASE-Grid Soil Moisture, Version 4*. [Online]. Available: https://nsidc.org/data/SPL3SMP/versions/4
[53] A. Colliander et al., "Validation of soil moisture data products from the NASA SMAP mission," *IEEE J. Sel. Topics Appl. Earth Observ. Remote Sens.*, vol. 15, pp. 364–392, 2022.
[54] M. Abdelkader et al., "Assessing the spatiotemporalvariability of smap soil moisture accuracy in a deciduous forestregion," *Remote Sensing*, vol. 14, no. 14, pp. 1–12, 2022. [Online]. Available: https://www.mdpi.com/2072-4292/14/14/3329
[55] M. Friedl and D. Sulla-Menashe, "MCD12C1 MODIS/Terra Aqua land cover type yearly L3 global 0.05deg CMG v006," NASA Land Processes Distrib. Act. Arch. Center (LP DAAC), Sioux Falls, SD, USA, Tech. Rep., 2015.



Erik Hodges (Member, IEEE) received the B.S. degree in electrical engineering from the University of California at Los Angeles, Los Angeles, CA, USA, in 2019. He is currently pursuing the Ph.D. degree in electrical engineering with the University of Southern California, Los Angeles.

He is a member of the Cyclone Global Navigation Satellite System science team. His research interests include global navigation satellite system reflectometry and electromagnetic models for land surfaces.

Mr. Hodges is a member of the IEEE Geoscience and Remote Sensing Society.



Clara Chew (Member, IEEE) received the B.A. degree in environmental studies from Dartmouth College, Hanover, NH, USA, in 2009, and the Ph.D. degree in geology from the University of Colorado, Boulder, CO, USA, in 2015.

She is a Terrestrial Hydrologist who specializes in soil moisture remote sensing.



Eric E. Small (Member, IEEE) received the B.A. degree in geological sciences from the Williams College, Williamstown, MA, USA, in 1993 and the Ph.D. degree in Earth sciences from the University of California at Santa Cruz, Santa Cruz, CA, USA, in 1998.

He is currently a Professor with the Department of Geological Sciences, University of Colorado, Boulder, CO, USA. His research is focused on land surface hydrology.



Dinan Bai (Member, IEEE) received the B.S. degree (Hons.) in electrical and computer engineering from The Ohio State University, Columbus, OH, USA, in 2022, and the M.S. degree in electrical and computer engineering from the University of Michigan, Ann Arbor, MI, USA, in 2024, where he is currently pursuing the Ph.D. degree with the Department of Climate and Space Science and Engineering.

Since 2022, he has been a Graduate Research Assistant with the Remote Sensing Group, Department of Climate and Space Science and Engineering, University of Michigan. His research interests include applied electromagnetics, microwave remote sensing system design, calibration, and applications.



Mohammad Al-Khaldi (Member, IEEE) received the bachelor's degree in electrical engineering from American University of Sharjah, Sharjah, United Arab Emirates, in 2015, the M.S. degree in electrical engineering from Texas A&M University, College Station, TX, USA, in 2017, the M.S. degree in electrical and computer engineering from The Ohio State University, Columbus, OH, USA, in 2019, and the Ph.D. degree from the Department of Electrical and Computer Engineering and the ElectroScience Laboratory, The Ohio State University, in 2020.

He was a Project Scientist I, a Post-Doctoral Fellow II, and a Post-Doctoral Fellow I at the University Corporation for Atmospheric Research's (UCAR's) COSMIC Program, Boulder, CO, USA. He is currently a Research Scientist at the ElectroScience Laboratory and the Department of Electrical and Computer Engineering, The Ohio State University. He is a member of the NASA CYGNSS Mission science team and the NASA CYGNSS Mission Calibration and Validation Team, and a NASA CSDA GNSS-R Subject Matter Expert (SME). His research interests include applied electromagnetics, rough surface scattering, and spaceborne remote sensing.

Dr. Al-Khaldi is a member of the IEEE GRSS Technical Committee on Modeling in Remote Sensing and the IEEE GRSS Technical Committees on Frequency Allocations in Remote Sensing and an Associate Member of Commissions B and F of the International Union of Radio Science (URSI). He serves as an Associate Editor for *Radio Science*.

Authorized licensed use limited to: University of Michigan Library. Downloaded on August 28,2025 at 02:12:38 UTC from IEEE Xplore. Restrictions apply.



Jeffrey D. Ouellette (Member, IEEE) received the B.Sc. degree in electrical engineering from the Western New England College, Springfield, MA, USA, in 2010, and the M.Sc. and Ph.D. degrees in electrical engineering from The Ohio State University, Columbus, OH, USA, in 2013 and 2015, respectively.

He was a NASA Earth and Space Science Fellow from 2013 to 2015. He is currently an Electronics Engineer at the Remote Sensing Division, U.S. Naval Research Laboratory (NRL), Washington, DC, USA, having entered federal service in 2015 under as a Karles Fellow. He is presently listed as a lead author or the co-author on more than 35 publications in academic journals and conference proceedings. His professional experience and research interests include electromagnetic scattering theory, passive radar hardware and software design, microwave remote sensing retrieval algorithm development and implementation, and calibration/validation of microwave remote sensing data products.

Dr. Ouellette is a member of the Union Radio-Scientifique Internationale (Commission F) and received the Alan Berman Research Publication Award in 2021.



Joel T. Johnson (Fellow, IEEE) received the Bachelor of Electrical Engineering degree from Georgia Institute of Technology, Atlanta, GA, USA, in 1991, and the S.M. and Ph.D. degrees from Massachusetts Institute of Technology, Cambridge, MA, USA, in 1993 and 1996, respectively.

He is currently the Burn and Sue Lin Professor with the Department of Electrical and Computer Engineering and the ElectroScience Laboratory, The Ohio State University, Columbus, OH, USA. His research interests are in the areas of microwave remote sensing, propagation, and electromagnetic wave theory.

Dr. Johnson is a member of Commissions B and F of the International Union of Radio Science (URSI), Tau Beta Pi, Eta Kappa Nu, and Phi Kappa Phi. He received the 1993 Best Paper Award from the IEEE Geoscience and Remote Sensing Society. He was named an Office of Naval Research Young Investigator, a National Science Foundation Career awardee, and a PECASE award recipient in 1997. He was recognized by U.S. National Committee of URSI as a Booker Fellow in 2002. He currently serves as the Deputy Editor-in-Chief for IEEE TRANSACTIONS ON GEOSCIENCE AND REMOTE SENSING.



Fangni Lei received the B.S. degree in geographic information systems and the M.S. and Ph.D. degrees in cartography and geographical information engineering from Wuhan University, Wuhan, China, in 2011, 2013, and 2016, respectively.

She was a Visiting Student with the Hydrology and Remote Sensing Laboratory, USDA-Agricultural Research Services, Washington, DC, USA. She continued her research as a Post-Doctoral Associate with USDA, Washington, from 2017 to 2019 and then as a Research Assistant Professor with Mississippi State University, Starkville, MS, USA, from 2019 to 2022. She is currently an Assistant Research Professor with the Eversource Energy Center and the Department of Civil and Environmental Engineering, University of Connecticut, Storrs, CT, USA. Her research interests include but are not limited to quantifying soil moisture from microwave remote sensing, land surface water–energy balance modeling, watershed-scale hydrologic modeling, hydrologic data assimilation, and agricultural water management.



Mehmet Kurum (Senior Member, IEEE) received the B.S. degree in electrical and electronics engineering from Boğaziçi University, Istanbul, Türkiye, in 2003, and the M.S. and Ph.D. degrees in electrical engineering from George Washington University, Washington, DC, USA, in 2005 and 2009, respectively.

He held post-doctoral and research associate positions at the Hydrological Sciences Laboratory, NASA Goddard Space Flight Center, Greenbelt, MD, USA. From 2016 to 2022, he was an Assistant Professor with Mississippi State University (MSU), Starkville, MS, USA, and subsequently, he held the position of an Associate Professor and the Paul B. Jacob Endowed Chair until 2023. He is currently an Associate Professor of electrical and computer engineering with the University of Georgia, Athens, GA, USA, and an Adjunct Professor with MSU. His research focuses on recycling the radio spectrum to address the challenges of decreasing radio spectrum space for science while exploring entirely new microwave regions for land remote sensing.

Dr. Kurum is a Senior Member of the IEEE Geoscience and Remote Sensing Society and a member of U.S. National Committee for the International Union of Radio Science. He was a recipient of the Leopold B. Felsen Award for Excellence in Electromagnetic in 2013, the URSI Young Scientist Award in 2014, and the NSF CAREER Award in 2022. He has been an Associate Editor of IEEE TRANSACTIONS ON GEOSCIENCE AND REMOTE SENSING and IEEE JOURNAL OF SELECTED TOPICS IN APPLIED EARTH OBSERVATIONS AND REMOTE SENSING since 2021. From 2014 to 2021, he was an Early Career Representative for the International URSI Commission F (Wave Propagation and Remote Sensing).



Ali Cafer Gurbuz (Senior Member, IEEE) received the B.S. degree in electrical engineering from Bilkent University, Ankara, Türkiye, in 2003, and the M.S. and Ph.D. degrees from Georgia Institute of Technology, Atlanta, GA, USA, in 2005 and 2008, respectively, both in electrical and computer engineering.

Prior to joining North Carolina State University, Raleigh, NC, USA, he was a Post-Doctoral Fellow at Georgia Institute of Technology and held assistant and associate professor positions at Mississippi State University, Starkville, MS, USA. His research interests include signal/image processing and machine learning for radar, remote sensing, and wireless communication applications; compressive sensing; physics aware and explainable machine learning for inverse problems; computational imaging; multisensor activity sensing; radar/communication coexistence; passive sensing; autonomous aerial vehicle-based remote sensing, and precision agriculture.

Dr. Gurbuz is a National Science Foundation Faculty Early Career Development (CAREER) Awardee and a Turkish Academy of Sciences Best Young Scholar. He is currently an Associate Editor of IEEE TRANSACTIONS ON AEROSPACE AND ELECTRONIC SYSTEMS.



Volkan Senyurek received the B.S., M.S., and Ph.D. degrees in electronics and communication engineering from Marmara University, Istanbul, Turkey, in 2003, 2007, and 2013, respectively.

After he completed his Ph.D. degree, he worked as an Assistant Professor at Marmara University until 2015. From 2015 to 2017, he worked as a Post-Doctoral Researcher at the Department of Mechanical and Materials Engineering, Florida International University, Miami, FL, USA. From 2017 to 2019, he was with the Department of Electric and Computer Engineering, The University of Alabama, Tuscaloosa, AL, USA, as a Post-Doctoral Researcher. Currently, he is an Assistant Research Professor at the Geosystems Research Institute, Mississippi State University, Starkville, MS, USA. His research interests are remote sensing for precision agriculture, biomedical signal processing, wearable sensors, pattern recognition, and structural health monitoring.

Authorized licensed use limited to: University of Michigan Library. Downloaded on August 28,2025 at 02:12:38 UTC from IEEE Xplore. Restrictions apply.



M. M. Nabi received the bachelor's degree in electrical and electronics engineering from the Ahsanullah University of Science and Technology, Dhaka, Bangladesh, in 2014, the master's degree in information technology from the University of Dhaka, Dhaka, in 2016, and the Ph.D. degree in electrical and computer engineering from Mississippi State University (MSU), Starkville, MS, USA, in 2024.

He has been working as a Graduate Research Assistant at the High-Performance Computing Collaboratory (HPCC) and the Information Processing and Sensing (IMPRESS) Laboratory, MSU. Currently, he is an Assistant Professor with the School of Engineering and Applied Science, Western Kentucky University, Bowling Green, KY, USA. His research interests include signal processing, remote sensing, machine learning, and deep learning.



Xiaolan Xu (Senior Member, IEEE) received the B.Eng. degree from Zhejiang University, Hangzhou, China, in 2006, and the M.S. and Ph.D. degrees in electrical engineering from the University of Washington, Seattle, WA, USA, in 2008 and 2011, respectively.

She began as a Post-Doctoral Researcher at the Science Division (329F) and transitioned to a Scientist role in 2014. She has established expertise in modeling microwave signal interactions (active, passive, and bistatic) with the Earth's surface, focusing on hydrological applications such as soil moisture retrieval and snow water equivalence estimation. Her significant contributions to the SMAP mission, the Signals of Opportunity (SoOp) Community, and collaborations on topographic snow radar technologies highlight her innovative research approach.

Dr. Xu was a recipient of the Union Radio-Scientifique Internationale (URSI) Awards for 2020 Santimay Basu Prize.



Rashmi Shah (Senior Member, IEEE) received the B.S. degree in electrical engineering from Rochester Institute of Technology, Rochester, NY, USA, in 2007, and the M.S. and Ph.D. degrees in aeronautical and astronautical engineering from Purdue University, West Lafayette, IN, USA, in 2010 and 2014, respectively.

Since 2014, she has been at Jet Propulsion Laboratory (JPL), Tracking Systems and Applications Section, California Institute of Technology (Caltech), Pasadena, CA, USA, as a Research Technologist. Her background and interests are microwave remote sensing, electromagnetic scattering, remote sensing using signals of opportunity reflectometry, and microwave remote sensing instrument development.



Simon H. Yueh (Fellow, IEEE) received the Ph.D. degree in electrical engineering from Massachusetts Institute of Technology, Cambridge, MA, USA, in January 1991.

He was a Post-Doctoral Research Associate at Massachusetts Institute of Technology from February to August 1991. In September 1991, he joined the Radar Science and Engineering Section, Jet Propulsion Laboratory (JPL), California Institute of Technology (Caltech), Pasadena, CA, USA. He was the Supervisor of the Radar System Engineering and Algorithm Development Group from 2002 to 2007, the Deputy Manager of the Climate, Oceans and Solid Earth Section from July 2007 to March 2009, and the Section Manager from April 2009 to January 2013. He served as the Project Scientist of the National Aeronautics and Space Administration (NASA) Aquarius Mission from January 2012 to September 2013, the Deputy Project Scientist of NASA Soil Moisture Active Passive Mission from January 2013 to September 2013, and the SMAP Project Scientist since October 2013. He has been the Principal/Co-Investigator of numerous NASA and DOD research projects on remote sensing of ocean salinity, ocean wind, terrestrial snow, and soil moisture. He has authored four book chapters and published more than 300 publications and presentations.

Dr. Yueh is a member of URSI Commission F. He received the 2021 IEEE J-STARS Prize Paper Award, the 2014 IEEE GRSS Transaction Prize Paper Award, the 2010 IEEE GRSS Transaction Prize Paper Award, the 2002 IEEE GRSS Transaction Prize Paper Award, the 2000 Best Paper Award in the IEEE International Geoscience and Remote Symposium 2000, the 1995 IEEE GRSS Transaction Prize Paper Award for a paper on polarimetric radiometry, the JPL Lew Allen Award in 1998, the Ed Stone Award in 2003 and 2023, and the IEEE GRSS Service Award in 2023. He was an Associate Editor of *Radio Science* from 2002 to 2006 and the Editor-in-Chief of IEEE TRANSACTIONS ON GEOSCIENCE AND REMOTE SENSING from 2018 to 2022.



Akiko Hayashi received the B.S. degree in civil engineering and the M.S. degree in structural engineering from Duke University, Durham, NC, USA, in 1982 and 1984, respectively.

After graduation, she was with the Structures and Dynamics Technology Group, Jet Propulsion Laboratory (JPL), California Institute of Technology, Pasadena, CA, USA, where she was engaged in structural analysis and finite element modeling. In 1988, she moved to the Oceanography Group and worked on altimetry data. She is currently a member of the Oceans and Ice Group, JPL, working on altimetry data from Ocean Surface Topography Mission/Jason-2, ocean salinity data from Aquarius, Soil Moisture Active Passive data, and CYGNSS.



Paulo T. Setti Jr. received the B.E. degree in geomatics and the M.Sc. degree in cartographic sciences from São Paulo State University, Presidente Prudente, Brazil, in 2017 and 2019, respectively, and the Ph.D. degree in engineering sciences from the University of Luxembourg, Esch-sur-Alzette, Luxembourg, in 2023.

He is currently a Post-Doctoral Researcher with the Geophysics and Remote Sensing Laboratory, University of Luxembourg. His research interests include unconventional applications of satellite geodesy for earth observation, global navigation satellite system (GNSS) reflectometry, and mitigation of ionospheric effects on multiconstellation GNSS positioning.

Authorized licensed use limited to: University of Michigan Library. Downloaded on August 28,2025 at 02:12:38 UTC from IEEE Xplore. Restrictions apply.



Sajad Tabibi received the M.Sc.Eng. degree in geodesy from the K. N. Toosi University of Technology, Tehran, Iran, in 2010, and the Ph.D. degree in engineering sciences from the University of Luxembourg, Esch-sur-Alzette, Luxembourg, in 2016.

He has been a full-time Faculty Member with the Geophysics and Remote Sensing (GRS) Laboratory, University of Luxembourg, since 2016. His research interests include remote sensing through innovative applications of satellite geodesy, global navigation satellite system-reflectometry, and sensor technology development for environmental applications.



Emanuele Santi (Senior Member, IEEE) received the M.S. degree in electronic engineering from the University of Florence, Florence, Italy, in 1997, and the Ph.D. degree in Earth's remote-sensing techniques from the University of Basilicata, Potenza, Italy, in 2005.

Since 1998, he has been with the Microwave Remote Sensing Group, Institute of Applied Physics, National Research Council, Florence, where he got a permanent staff position in 2009 and a senior researcher position in 2023 and became a member of the Institute Advisory Board in 2024. He was and is currently involved in many national and international projects funded by Italian Space Agency (ASI), European Community (EC), European Space Agency (ESA), and Japanese Aerospace Exploration Agency (JAXA), acting as a Team Leader, a WP Leader, and a Co-Investigator. He is an external scientist of NASA's CYGNSS science team and a member of the ESA's HydroGNSS science team with responsibility for forest biomass product development and involved in JAXA's GCOM science team. He has authored or co-authored 194 articles and published in ISI journals and books and conference proceedings (source Scopus—H-index 27). His research interests include the development and validation of models and inversion algorithms based on machine learning for estimating the geophysical parameters of soil, sea, snow, and vegetation from microwave emission and scattering.

Dr. Santi won the IEEE GRSS J-STARS Prize Paper Award for the best paper published on IEEE JOURNAL OF SELECTED TOPICS IN APPLIED EARTH OBSERVATIONS AND REMOTE SENSING in 2018. He is the Chair of the IEEE GRS chapter CNI-29 and the SPIE Europe Remote Sensing conference RS-106 and is a member of the Steering Committee of the "Centro di Telerilevamento a Microonde" (Microwave Remote Sensing Center). In 2020, he served as the Chair for the 16th Symposium on Microwave Radiometry MicroRad.



Simone Pettinato (Member, IEEE) received the M.S. degree in telecommunications engineering from the University of Florence, Florence, Italy, in 2002, and the Ph.D. degree in "methods and technologies for environmental monitoring" from the University of Basilicata, Potenza, Italy, in 2007.

Since 2003, he worked at the Microwave Remote Sensing Group, National Research Council (CNR)–IFAC, Florence, as a Scientist. In the end of 2013, he took on a permanent position, and in 2023, he became a Senior Researcher. The objective of his research consists mainly of the investigation of the natural surfaces by means of active and passive microwave sensors, in order to retrieve information on soil moisture, snow, and vegetation biomass. He gained experience in satellite data processing of synthetic aperture radar (SAR), microwave radiometers, and multispectral images. He is specialized in comparing ground data with satellite data with the aim of verifying the sensitivity of SAR satellite data to land parameters. He participated, as co-investigator, in several international scientific projects funded by the European Community and European Space Agency (ESA). In 2009, 2010, and 2012, he was involved in three Antarctic expeditions managed by Italian national research program in order to allow the execution of the DOMEX-2, DOMEX-3, and GPS-SIDS projects. He was involved in Italian Space Agency (ASI) projects aimed at the use of X-, C-, and L-band SAR data for the development of biomass, soil moisture, and snow estimation algorithms. He is involved with the ESA HYDROGNSS project. In 2023 and 2024, he was a Professor on contract at Pavia University, Pavia, Italy, teaching microwave remote sensing applications. He is the author or co-author of more than 140 papers published in international peer-reviewed journals and conference proceedings.

Dr. Pettinato is a reviewer of IEEE TRANSACTIONS ON GEOSCIENCE AND REMOTE SENSING, JSTARS, and MDPI journals.



Christopher S. Ruf (Life Fellow, IEEE) received the B.A. degree in physics from the Reed College, Portland, OR, USA, in 1982, and the Ph.D. degree in electrical and computer engineering from the University of Massachusetts at Amherst, Amherst, MA, USA, in 1987.

He has worked previously with Intel Corporation, Santa Clara, CA, USA, Hughes Space and Communication, Aurora, CO, USA, the NASA Jet Propulsion Laboratory, Pasadena, CA, USA, and Penn State University, State College, PA, USA. He is currently the Frederick Bartman Collegiate Professor of Climate and Space Science and the Director of the Space Institute, University of Michigan, Ann Arbor, MI, USA, and a Principal Investigator of the NASA CYGNSS Mission. His research interests include remote sensing methods, applications, and technology.

Prof. Ruf is a fellow of American Meteorological Society, the Vice Chair of Commission F of U.S. National Committee for the Union Radio Scientifique Internationale, and a member of American Geophysical Union. He is former Editor-in-Chief of IEEE TRANSACTIONS ON GEOSCIENCE AND REMOTE SENSING and has served on the Editorial Board of *Radio Science*, *Journal of Atmospheric and Oceanic Technology*, and *Scientific Reports*.



Mahta Moghaddam (Fellow, IEEE) received the B.S. degree (Hons.) in electrical and computer engineering from The University of Kansas, Lawrence, KS, USA, in 1986, and the M.S. and Ph.D. degrees in electrical and computer engineering from the University of Illinois at Urbana–Champaign, Urbana, IL, USA, in 1989 and 1991, respectively.

She is a Distinguished Professor and the holder of the Ming Hsieh Chair with the Department of Electrical and Computer Engineering, University of Southern California, Los Angeles, CA, USA. Prior to that, she was a Professor of electrical and computer engineering at the University of Michigan, Ann Arbor, MI, USA, from 2003 to 2011, and NASA Jet Propulsion Laboratory (JPL), Pasadena, CA, USA, from 1991 to 2003. She has introduced new approaches for quantitative interpretation of multichannel radar imagery based on analytical inverse scattering techniques applied to complex and random media. She was a System Engineer for the Cassini Radar and was the Science Chair of the JPL Team X (Advanced Mission Studies Team). She was the Principal Investigator of the AirMOSS NASA Earth Ventures 1 Mission and is a member of the National Academy of Engineering. Her most recent research interests include the development of new radar instrument and measurement technologies for subsurface and subcanopy characterization, development of forward and inverse scattering techniques for layered random media especially for soil moisture and permafrost applications, geophysical retrievals using signal-of-opportunity reflectometry, and transforming concepts of radar remote sensing to medical imaging and therapy systems.

Dr. Moghaddam was a member of the SMAP Mission Science Team and is a member of the CYGNSS science team.

Authorized licensed use limited to: University of Michigan Library. Downloaded on August 28,2025 at 02:12:38 UTC from IEEE Xplore. Restrictions apply.